Available online at www.sciencedirect.com
SCIENCE DIRECT®
Biochimica et Biophysica Acta 1612 (2003) 52–58
BIOCHIMICA ET BIOPHYSICA ACTA
BBA
www.bba-direct.com

Investigating magnetically aligned phospholipid bilayers with various lanthanide ions for X-band spin-label EPR studies

Marc A. Caporini, Arun Padmanabhan, Thomas B. Cardon, Gary A. Lorigan *

Department of Chemistry and Biochemistry, College of Arts and Science, Miami University, Oxford, OH 45056-1465, USA

Received 29 July 2002; received in revised form 19 February 2003; accepted 27 February 2003

Abstract

This paper reports the EPR spectroscopic characterization of a model membrane system that magnetically aligns with a variety of different lanthanide ions in the applied magnetic field (< 1 T) of an X-band EPR spectrometer. The ability to align phospholipid bilayer systems is valuable because the anisotropic spectra provide a more detailed and complete description of the structural and motional properties of the membrane-associated spin label when compared to randomly dispersed EPR spectra. The nitroxide spin probe 3β-doxyl-5α-cholestane (cholestane or CLS) was inserted into the bilayer discs to demonstrate the effects of macroscopic bilayer alignment through the measurement of orientational dependent hyperfine splittings. The effects of different lanthanide ions with varying degrees of magnetic susceptibility anisotropy and relaxation properties were examined. For X-band EPR studies, the minimal amounts of the Tm^{3+}, Yb^{3+}, and Dy^{3+} lanthanide ions needed to align the phospholipid bilayers were determined. Power saturation EPR experiments indicate that for the sample compositions described here, the spin-lattice relaxation rate of the CLS spin label was increased by varying amounts in the presence of different lanthanide (Gd^{3+}, Dy^{3+}, Er^{3+}, Yb^{3+}, and Tm^{3+}) ions, and in the presence of molecular oxygen. The addition of Gd^{3+} caused a significant increase in the spin-lattice relaxation rate of CLS when compared to the other lanthanide ions tested.

Keywords: Model membrane; Nitroxide spin label; EPR spectroscopy; Magnetically oriented; Membrane protein

1. Introduction

The utilization of aligned model membranes in both NMR [1–11] spectroscopy and EPR [12–14] spectroscopy has provided a wealth of structural and dynamic information about membrane associated molecules. The orientational dependent behavior of various nitroxide spin labels incorporated into aligned membrane systems has been investigated by several researchers with EPR spectroscopy [12–21]. Membrane alignment is usually carried out using two methods: (1) mechanical orientation on glass plates or mylar films and (2) the isopotential spin-dry ultracentrifugation (ISDU) technique [13,20]. In aligned phospholipid bilayer samples, the resulting EPR spectra reveal orientational dependent changes in the hyperfine splitting based upon the alignment of the spin label with respect to the magnetic field as well as a reduction in the spectral line widths. Reduced line widths improve spectral resolution and enable the ^{14}N hyperfine splitting and g tensors to be measured with greater precision. The anisotropic hyperfine splitting of aligned spin-labeled phospholipid bilayers can provide a more detailed structural picture of the probe with respect to the membrane when compared to randomly dispersed phospholipid bilayer samples. Also, molecular motions can be probed over a broad range of frequencies by examining aligned spin-labeled membrane systems at variable resonant microwave frequencies [12,18]. Thus, structural and dynamic information can be gleaned from the EPR spectrum of oriented spin-labeled phospholipid bilayers to provide a more detailed understanding of complex biological membranes at the molecular level.

Membrane systems that spontaneously align in magnetic fields have been demonstrated to be successful for a wide range of NMR studies for membrane and integral membrane proteins and peptides [2,6,10,11,22–28]. These oriented membrane systems are composed of a mixture of a bilayer-forming phospholipid and a short-chain phospholipid that

* Corresponding author. Tel.: +1-513-529-3338; fax: +1-513-529-5715.
E-mail address: lorigag@muohio.edu (G.A. Lorigan).

0005-2736/03/$ - see front matter © 2003 Elsevier Science B.V. All rights reserved.
doi:10.1016/S0005-2736(03)00085-3

breaks up the extended bilayers into bilayered micelles or bicelles that are highly hydrated (approximately 75% aqueous). Generally, the lipid mixture consists of long-chain bilayer-forming 1,2-dimyristoyl-*sn*-glycero-3-phosphocholine (DMPC) phospholipids and short-chain 1,2-dihexanoyl-*sn*-glycero-3-phosphocholine (DHPC) phospholipids. The *q*-ratio (DMPC/DHPC) between the two phospholipids is used to define the structural geometry of the bicelle [22,29]. The morphology of the magnetically aligned phospholipid micelles (bicelles) has been described as disc-like with approximate dimensions of 200 × 40 Å depending upon the long-chain/short-chain lipid ratio and the temperature [29].

The magnetic alignment of bicelles is due to the anisotropy of the overall magnetic susceptibility of the system. The negative sign of the diamagnetic susceptibility anisotropy tensor ($\Delta\chi < 0$) for phospholipid bilayers dictates that the bicelles align with their bilayer normal oriented perpendicular to the direction of the static magnetic field [22]. The addition of paramagnetic lanthanide ions with large positive magnetic susceptibilities (Eu^{3+}, Er^{3+}, Tm^{3+}, and Yb^{3+}) can cause the bicelles to flip 90° such that the average bilayer normal is colinear with the direction of the static magnetic field [23]. The ions are thought to associate with the phospholipid headgroups of the bicelles, changing the overall $\Delta\chi$.

Although bicelle model membrane systems were initially developed for NMR applications, it has been noted that bicelles hold promise for being well-suited for a wide variety of other biophysical applications such as neutron diffraction, X-ray diffraction, EPR spectroscopy, and several optical spectroscopic techniques [10,30]. In this paper, we extend upon our previous work and describe the effect that different lanthanide ions have on magnetically aligned and randomly dispersed phospholipid bilayers for spin-labeled X-band EPR spectroscopic studies [31,32]. The development of this new spin-label method will open up a whole new area of investigation for phospholipid bilayer systems and membrane protein EPR studies.

2. Materials and methods

2.1. Sample preparation

DMPC, DHPC, and 1,2-dimyristoyl-*sn*-glycero-3-phosphoethanolamine-*N*-[methoxy-(polyethylene glycol)-2000] (PEG2000-PE) were purchased from Avanti Polar Lipids (Alabaster, AL). Thulium (III) chloride hexahydrate, dysprosium (III) chloride hexahydrate, erbium (III) chloride hexahydrate, ytterbium (III) chloride hexahydrate, gadolinium (III) chloride hexahydrate, cholestane, and *N*-[2-hydroxyethyl]piperazine-*N*′-[2-ethanesulfonic acid] (HEPES) were obtained from Sigma/Aldrich. The cholesterol was obtained from Avocado Research Chemicals, Ltd. All lipids were dissolved in chloroform and stored at −20 °C prior to use. Aqueous solutions of lanthanide ions were prepared fresh each day. All aqueous solutions were prepared with nanopure filtered water.

The standard bicelle sample, consisting of 25% (w/w) phospholipid to solution with a $q = 3.5$, was made in 15- or 25-ml pear-shaped flasks. In the flask DMPC, PEG2000-PE, DHPC, cholesterol, and cholestane were mixed in ratios of 3.5:0.035:1:0.35:0.0196, respectively. The chloroform in the flask was rotovaped off using a Buchi R-3000 rotovap (approximately 20 min), and the flask was placed under high vacuum overnight.

The following day, an appropriate amount of 100 mM HEPES buffer at pH 7.0 was added to the flask. The flask was then vortexed briefly, sonicated for about 30 min, and vortexed again. The samples were sonicated with a Fisher Scientific FS30 bath sonicator (Florence, KY) with the heater turned off. Occasionally, brief (10–20 s) cooling in an ice water bath was needed to remove all of the material from the sides and bottom of the flask. The combined sample was subjected to two freeze (77 K)/thaw (room temperature) cycles to homogenize the sample and remove any air bubbles. Finally, at 0 °C (ice bucket), an appropriate aliquot of a concentrated aqueous solution of lanthanide ion was added and mixed into the sample. Typically, the total mass of the prepared samples was 200 mg.

The bicelle samples were drawn into 1-mm ID capillary tubes (Kimax) via a syringe. Both ends of the capillary tube were sealed with Critoseal (Fisher Scientific) and placed inside standard quartz EPR tubes (Wilmad, 707-SQ-250 M) filled with light mineral oil.

2.2. EPR spectroscopy

All EPR experiments were carried out on a Bruker EMX X-band CW-EPR spectrometer consisting of an ER 041XG microwave bridge and a TE_{102} cavity coupled with a BVT 3000 nitrogen gas temperature controller (temperature stability of ± 0.2 °C). All EPR spectra were gathered with a center field of 0.3350 T, sweep width of 100 G, a microwave frequency of 9.39 GHz, modulation frequency of 100 kHz, modulation amplitude of 0.1 mT (pp), and a power of 6.3 mW (except for the power saturation studies). All oriented samples were aligned by warming the sample from 298 to 318 K at a maximum magnetic field strength of 0.64 T [32]. All of the EPR spectra and resulting graphs were processed on a 300 MHz G3 Macintosh computer utilizing the Igor software package (Wavemetrics, Lake Oswego, OR).

The DMPC-rich bilayer samples for the CW-EPR power saturation experiments were prepared with various lanthanide ions (Gd^{3+}, Dy^{3+}, Er^{3+}, Yb^{3+}, and Tm^{3+}) at a concentration of 20% (mol% lanthanide to DMPC), and in the presence or absence of O_2. Samples with O_2 were prepared by exposing the samples to air for at least 20 min before gathering the spectra. Degassed samples (absence of O_2) were prepared by bubbling N_2 gas through the HEPES buffer solution for approximately 20 min. Next, the degassed solution was

transferred to the pear-shaped flask containing the phospholipids and sealed with a rubber septum. Under a N_2 atmosphere, the sample was vortexed, sonicated, and subjected to freeze/thaw cycles as described above. Finally, N_2 gas was blown over the sample for at least 20 min and the sample was drawn into the capillary tube as described previously.

Power saturation experiments were carried out by gradually increasing the microwave power from 0.2 to 200 mW for all samples. The peak-to-peak amplitude of the $m_1 = 0$ transition was measured according to procedures established in the literature [33]. Spectra recorded from the same sample over increasing microwave power were normalized to the same spin concentration at $P_0 = 1.30$ mW. The resulting saturation curves for different samples were then scaled to the same amplitude at P_0.

3. Results

The spin-labeled EPR spectra of 3β-doxyl-5α-cholestane (CLS or cholestane) incorporated into DMPC/DHPC/cholesterol phospholipid bilayer discs are displayed in Fig. 1 as a function of the concentration of Tm^{3+} at 318 K. At 0% and 5% molar Tm^{3+} with respect to DMPC, the EPR spectra (Fig. 1(A) and (B)) indicate that the bicelle discs are not aligned with respect to the direction of the static magnetic field. At 10% molar Tm^{3+} with respect to DMPC, the hyperfine splitting observed in the EPR spectrum of Fig. 1(C) is significantly reduced when compared to the EPR spectra in Fig. 1(A) and (B). CLS has been shown to align with its long axis parallel to the long axis of the phospholipids and undergoes rapid rotational motion ($R_\parallel$) about this axis. The nitroxide *y*-axis is nearly parallel to the long axis of the steroid-derived spin probe. Thus, the line shape and reduced hyperfine splitting observed in Fig. 1(C) indicate macroscopic orientation of the membrane bilayers such that their normals (and hence *y*-axis of associated cholestane spin labels) are nearly parallel with the static magnetic field. Additional DMPC/DHPC/cholesterol/Tm^{3+} bicelle EPR spectra were collected up to 25% molar Tm^{3+} with respect to DMPC (data not shown).

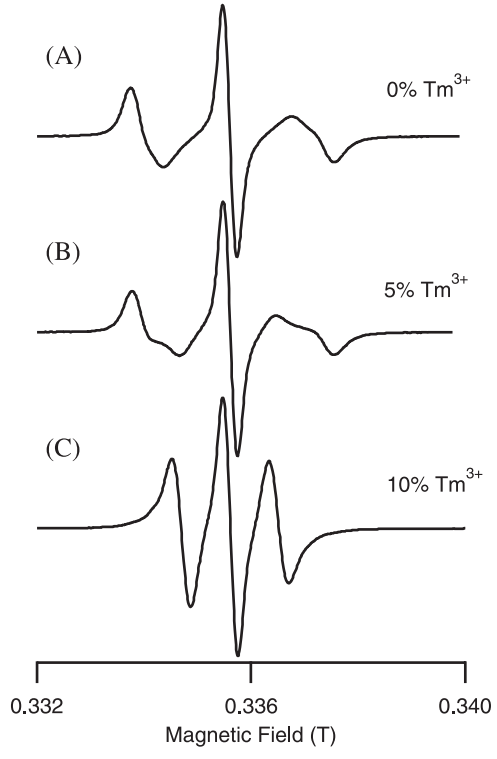

Fig. 1. EPR spectra of a cholestane spin label incorporated into oriented and randomly dispersed DMPC/DHPC/cholesterol phospholipid bilayers at concentrations of 0%, 5%, and 10% molar Tm^{3+} with respect to DMPC. Spectra were taken at 318 K and a static magnetic field strength of 0.64 T was used to align the samples. (A) 0% Tm^{3+} spectrum was typical of unoriented DMPC/DHPC phospholipid bilayers. (B) 5% Tm^{3+} spectrum showed some signs of parallel phospholipid bilayer alignment but remained mostly unaligned. (C) 10% Tm^{3+} spectrum revealed a fully aligned phospholipid bilayer system that was aligned such that the bilayer normal was colinear with the static magnetic field.

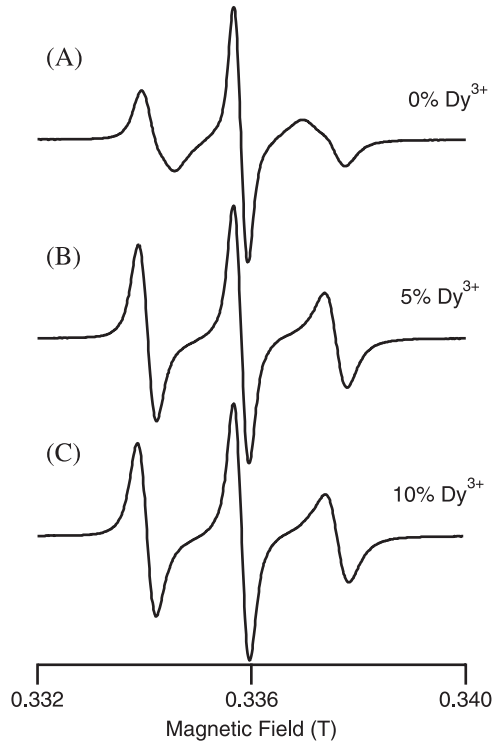

Fig. 2. EPR spectra of a cholestane spin label incorporated into oriented and randomly dispersed DMPC/DHPC/cholesterol phospholipid bilayers at concentrations of 0%, 5%, and 10% molar Dy^{3+} with respect to DMPC. Spectra were taken at 318 K and a static magnetic field strength of 0.64 T was used to align the samples. (A) 0% Dy^{3+} spectrum was typical of unoriented DMPC/DHPC phospholipid bilayers. (B) 5% Dy^{3+} spectrum indicated that the phospholipid bilayers were aligned such that the bilayer normal was perpendicular to the static magnetic field. (C) 10% Dy^{3+} spectrum indicated that the phospholipid bilayers were aligned such that the bilayer normal was perpendicular to the static magnetic field.

Similarly, Fig. 2 displays the EPR spectra of CLS incorporated into DMPC/DHPC/cholesterol phospholipid bilayers as a function of the concentration of Dy^{3+}. The

EPR spectrum displayed in Fig. 2(A) with 0% Dy^{3+} indicates that phospholipid bilayer arrays are randomly dispersed with respect to the direction of the static magnetic field. At the higher magnetic fields used in NMR studies, the phospholipid bilayered discs of this composition were aligned such that the membrane normal was perpendicular to the direction of the static magnetic field. At 0.3 T (X-band, $g=2$ resonance), additional lanthanide alignment reagents were needed to align the phospholipid bilayers [38].

Fig. 3 summarizes the results from Figs. 1 and 2 by showing the EPR spectroscopic data from a series of Tm^{3+} and Dy^{3+} bicelle titration experiments. The hyperfine splitting from various DMPC/DHPC bicelle samples was plotted versus the concentration of Tm^{3+} and Dy^{3+} with respect to DMPC.

In order to probe the effect that different lanthanide ions have on the electron spin-lattice relaxation rate of the cholestane spin label, a series of CW-EPR power saturation experiments were carried out on cholestane spin-labeled phospholipid bilayer samples in the presence and absence of oxygen at 318 K. Fig. 4 shows a series of power saturation curves for DMPC/DHPC/cholestane bicelle samples with Gd^{3+}, Dy^{3+}, and Tm^{3+} with and without O_2 compared to the control (no lanthanide, O_2 depleted). For all of the DMPC/DHPC samples, the normalized peak-to-peak amplitude of the $m_I=0$ transition was measured [33]. The power saturation curves for the various DMPC/DHPC samples are displayed as down triangles for the control sample, up triangles for the Gd^{3+} samples, squares for the Dy^{3+} samples, and circles for the Tm^{3+} samples. Saturation curves from samples prepared in the absence of O_2 are displayed as closed-face symbols, while samples prepared in the presence of O_2 are displayed as open-faced symbols.

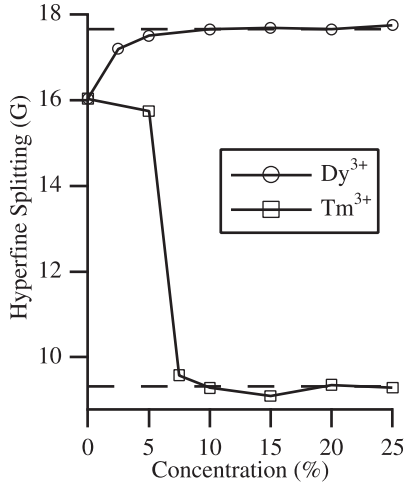

Fig. 3. Diagram showing the dependence of the hyperfine splitting on the concentration of Tm^{3+} and Dy^{3+} lanthanide ions added to DMPC/DHPC phospholipid bilayers. The squares represent the hyperfine splitting values measured from EPR spectra with Dy^{3+} and the circles are the resultant hyperfine splittings measured from EPR spectra with Tm^{3+}.

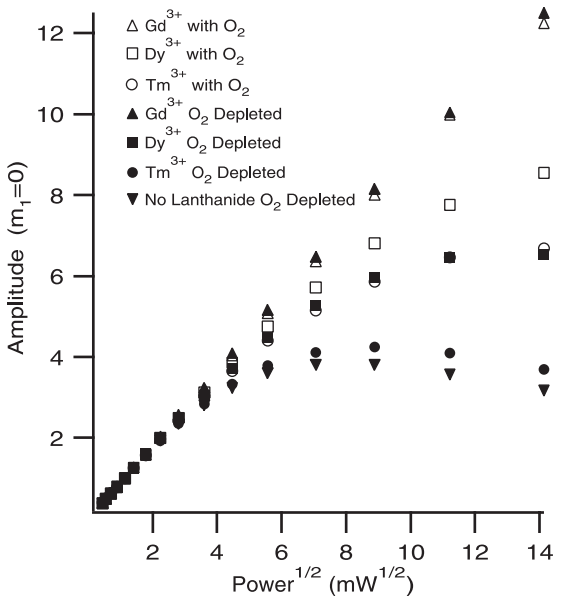

Fig. 4. EPR power saturation study of cholestane incorporated into DMPC/DHPC phospholipid bilayer samples with various lanthanide ions at 20% (mol% lanthanide to DMPC). Samples prepared with oxygen are shown with open-faced symbols, oxygen-depleted samples are shown with closed-faced symbols. The signal amplitude was measured from the peak-to-peak amplitude of the $m_I=0$ center line.

For comparison with a DMPC/DHPC bicelle model membrane system, similar CW-EPR power saturation studies were conducted on DHPC micelle samples. Fig. 5 shows a series of power saturation curves for DHPC micelle samples with and without oxygen and various different

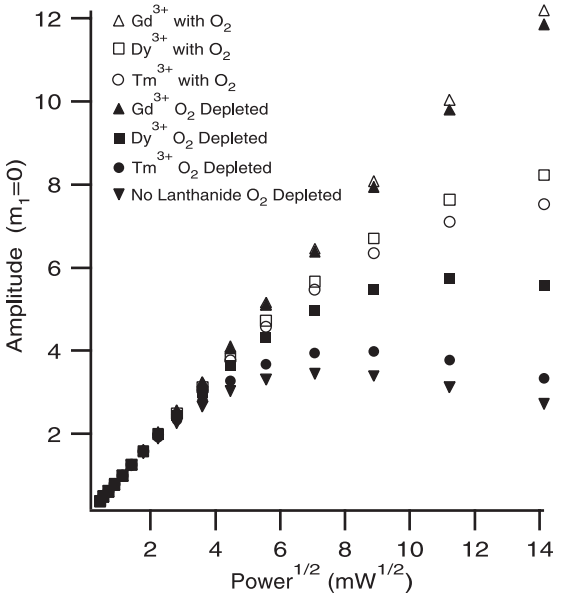

Fig. 5. EPR power saturation study of cholestane incorporated into DHPC micelles with various lanthanide ions at 20% (mol% lanthanide to DHPC). Samples prepared with oxygen are shown with open-faced symbols, oxygen-depleted samples are shown with closed-faced symbols. The signal amplitude was measured from the peak-to-peak amplitude of the $m_I=0$ center line.

Table 1
Power saturation parameters for various lanthanides ($\Delta P_{1/2}$)

Lanthanide	DHPC		DMPC/DHPC	
	(N_2)	(O_2)	(N_2)	(O_2)
Dy^{3+}	101	284	138	311
Er^{3+}	55.6	235	106	266
Yb^{3+}	20.4	192	42.2	227
Tm^{3+}	19.5	224	18.2	156

The $\Delta P_{1/2}$ values of both DMPC/DHPC bicelle and DHPC micelle samples with various lanthanides at 20% (mol% lanthanide to DMPC for bicelles, and DHPC for micelles) both with and without O_2. $\Delta P_{1/2}$ values for the bicelle samples were found by subtracting the $P_{1/2}$ of the control (DMPC/DHPC sample with no lanthanide and no O_2) from the $P_{1/2}$ of the sample. $\Delta P_{1/2}$ values for the micelle samples were found similarly, except a DHPC sample with no lanthanide and no O_2 was used as a control.

lanthanide ions (Gd^{3+}, Dy^{3+}, and Tm^{3+}). DHPC/cholestane samples are displayed as down triangles for the control sample, up triangles for the Gd^{3+} samples, squares for the Dy^{3+} samples, and circles for Tm^{3+} samples. The power saturation data arising from samples prepared in the presence of O_2 are shown as open-faced symbols; whereas, the curves arising from samples prepared in the absence of O_2 (O_2 depleted) are displayed as closed-faced symbols. As with the DMPC/DHPC samples, varying degrees of spin-lattice relaxation enhancement were observed for all of the lanthanide samples tested. The power saturation results for the DHPC micelle samples were comparable to the results from the DMPC/DHPC bicelle samples.

The saturation curves were then fitted to the function $A(P)=IP^{1/2}[1+(2^{1/\varepsilon}-1)P/P_{1/2}]^{-\varepsilon}$, where A is the peak-to-peak amplitude, P is microwave power, I is a scaling factor, ε is a measure of the inhomogeneity of the sample, and $P_{1/2}$ is the power at half saturation [33]. $\Delta P_{1/2}$ values for the bicelle samples were found by subtracting the $P_{1/2}$ of the control (DMPC/DHPC sample with no lanthanide and no O_2) from the $P_{1/2}$ of the sample. Table 1 shows the $\Delta P_{1/2}$ values ($P_{1/2}$(sample) − $P_{1/2}$(control)) for various lanthanide ions with (shown as O_2) and without O_2 (shown as N_2). The $\Delta P_{1/2}$ values for bicelle samples containing Gd^{3+} could not be determined due to the lack of saturation observed. The lanthanide samples showed varying degrees of $1/T_1$ enhancement as indicated by the increasing $\Delta P_{1/2}$ values, which was further enhanced by the addition of O_2.

4. Discussion

As illustrated in Fig. 1(C), magnetically aligned phospholipid bilayer samples doped with Tm^{3+} align such that the normal of the membrane bilayer is colinear with the direction of the static magnetic field. The preferred orientation of the bicelle disc director **n** in the presence of a magnetic field is dependent upon the sign of $\Delta\chi$ of the bicelle (the magnetic susceptibility anisotropy tensor of the bicelle disc). The sign of $\Delta\chi$ of the bicelle can be changed from negative to positive by adding paramagnetic lanthanide ions (i.e., Tm^{3+}, Yb^{3+}, Er^{3+}, Eu^{3+}) which bind to the phosphatidylcholine headgroups [23,34,35]. The magnitude and sign of $\Delta\chi$ for the bicelle are dependent upon the orientation of the principal magnetic axes of the lanthanide–phospholipid complex [36]. Inspection of the line shape and resultant hyperfine splitting in Fig. 1 indicates that the bicelle discs are not aligned at this orientation until 10% molar Tm^{3+} with respect to DMPC is added to the bicelle sample. Under identical alignment and magnetic field conditions, the phospholipid bilayer arrays do not fully align at this orientation until 15–20% molar Yb^{3+} with respect to DMPC is added to the bicelle matrix (data not shown). This is not surprising because the Tm^{3+} ion has the largest positive $\Delta\chi$ and should yield optimal alignment at lower concentrations when compared to Eu^{3+}, Er^{3+}, and Yb^{3+} ions which possess smaller positive $\Delta\chi$ values [23,24].

At the high magnetic fields typically used in NMR studies (greater than 7.0 T), the sign of $\Delta\chi$ for the bicelle discs is negative (in the absence of lanthanide ions). Thus, in the presence of a static magnetic field the preferred alignment of the bicelle disc director is oriented perpendicular to the applied magnetic field. For low field X-band EPR experiments (approximately 0.64 T), the phospholipid bilayer discs do not fully align at this orientation without additional alignment reagents [37]. Dy^{3+} ions must be added to the bicelle samples to align them at this orientation (Fig. 2(B) and (C)) [38]. The magnitude of the overall negative $\Delta\chi$ of the discs is increased by adding Dy^{3+} to the DMPC/DHPC bicelle matrix which alternatively possesses a large negative $\Delta\chi$ [23,24]. The resultant line shape and hyperfine splitting of the EPR spectra displayed in Fig. 2 indicate that the phospholipid bilayer arrays are aligned when only 5% molar Dy^{3+} with respect to DMPC is added to the sample.

Fig. 3 compares the resultant hyperfine splitting of CLS incorporated into DMPC/DHPC phospholipid bilayer arrays with varying Dy^{3+} and Tm^{3+} concentrations. The bicelle samples are almost fully aligned at 7.5% molar Tm^{3+} with respect to DMPC or at 2.5% molar Dy^{3+} with respect to DMPC as observed by the resultant line shape and hyperfine splitting. Complete bicelle disc alignment is observed at 10% molar Tm^{3+} or 5% molar Dy^{3+} with respect to DMPC. The data indicate that it takes approximately 50% less Dy^{3+} ions to align the bicelle discs at the perpendicular orientation when compared to Tm^{3+} ions in the parallel alignment. Less Dy^{3+} ions (which have a large negative $\Delta\chi$) are needed for alignment because the phospholipid bilayer arrays already possess a negative $\Delta\chi$; whereas a greater amount of Tm^{3+} ions (which have a smaller $|\Delta\chi|$ than Dy^{3+}) are needed to flip the bicelle discs by changing the magnitude and sign of $\Delta\chi$ for the bicelle system to a positive value. These results place a threshold on the minimal amount of lanthanide ions that are needed to align the DMPC/DHPC bilayers in the L_α phase for X-band EPR studies. The phospholipid bilayers in magnetically aligned bicelles are in the L_α phase at 318 K

and have the capacity to incorporate integral membrane proteins [22–24]. Thus, this study will be useful for investigating the structural and dynamical properties of membrane proteins with site-specific spin-labeled EPR studies with the smallest amount of paramagnetic lanthanide alignment reagents as possible to minimize potential protein–lanthanide ion interactions.

For complete and accurate analysis of spin-label EPR spectra collected for the magnetically aligned bicelle samples described here, the possible interfering effects of the paramagnetic lanthanide must be understood. A potential drawback of this system could be that the presence of the paramagnetic lanthanide that is required for sample alignment could cause significant paramagnetic line broadening and complicate detailed analysis of spin-label EPR spectra. We explored this possibility by performing power saturation studies on cholestane spin-labeled phospholipid bilayer samples (DMPC/DHPC) and also micelle samples (DHPC) with a variety of different lanthanide ions with and without oxygen at 318 K (Figs. 4 and 5, and Table 1). The addition of lanthanide ions increased the electron spin-lattice relaxation rate of the spin label as shown by the increase in $P_{1/2}$ values. The relaxation enhancement was the greatest for Gd^{3+}, which had a $\Delta P_{1/2}$ at least one order of magnitude larger than the other lanthanides because it was still in the linear region of the curve at all the power levels studied (Figs. 4 and 5). The $1/T_1$ of the spin label was increased by the other lanthanide ions with Dy^{3+} giving the greatest enhancement followed by Er^{3+}, Yb^{3+}, and Tm^{3+}. The addition of Tm^{3+} and Yb^{3+} ions to the bicelle samples caused a minimal change in $1/T_1$ of CLS. In the presence of paramagnetic O_2, the power required to saturate the cholestane spin label increased due to an enhancement of the spin-lattice relaxation rate ($1/T_1$) of the nitroxide electron [40–42]. The interaction of a nitroxide spin label with a paramagnetic species like molecular oxygen, which diffuses through the membrane and collides with the spin label, is dominated by Heisenberg spin exchange and yields changes in the electron spin-lattice relaxation rate of the spin label [43]. The data presented here suggest that the paramagnetic lanthanide ions used in the bicelle samples interact via an alternative relaxation mechanism. In phospholipid membranes, the positively charged lanthanide ions bind at the surface of the membrane and do not readily diffuse through the bilayer. The interaction between the positively charged lanthanide ions and the negative charges associated with the phospholipid head groups is believed to be electrostatic in nature and involves the formation of coordination complexes with one or more of the phosphate groups [35,39].

For two different paramagnetic species that do not undergo rapid collisions such as a paramagnetic ion and a nitroxide spin label separated by a distance r that is large enough to preclude orbital overlap, the relaxation interaction is governed by a dipolar mechanism [42,44–46]. The dipolar relaxation mechanism is proportional to $\mu_R^2 T_{1R}/r^6$, where μ_R and T_{1R} represent the magnetic moment and electron spin-lattice relaxation time of the transition ion probe. Thus, a paramagnetic species like Gd^{3+}, which possesses a large magnetic moment and a relatively long spin-lattice relaxation time, significantly alters the relaxation properties of the spin label. However, depending upon the magnitude of r, ions with shorter T_{1R} values such as Yb^{3+}, Dy^{3+}, Ho^{3+}, Er^{3+}, and Tm^{3+} will have less significant effects on the dipolar relaxation mechanism when compared to Gd^{3+} [42,46]. Gd^{3+} has a T_{1R} value of 1×10^{-8} s, whereas Tm^{3+} and Yb^{3+} have much shorter T_{1R} values of approximately 2.8×10^{-13} s [47,48]. Thus, the increased relaxation rates (observed through $\Delta P_{1/2}$ values) of the spin label caused by a particular lanthanide ion are correlated to the T_{1R} times, supporting the dipolar relaxation interaction with the lanthanides being bound to the surface of the bilayer and not coming in direct contact with the spin label. The development of magnetically aligned phospholipid bilayers utilizing lanthanide alignment reagents at low magnetic fields provides enormous potential for investigating membrane protein systems with spin-label EPR spectroscopy. A wide variety of spin labels including site-directed spin labels attached to integral membrane proteins or peptides, steroid derivatives, and fatty acid labels can be easily integrated into aligned phospholipid bicelle systems and studied via EPR spectroscopy. Thus, this new technique will enable the development of a more accurate and detailed understanding of complex biological mixtures found in membrane protein environments.

Acknowledgements

The X-band CW-EPR spectrometer was obtained from an NSF Grant (CHE-97,24192). GAL would like to acknowledge support for this work from an NSF CAREER Award (CHE-0133433) and an NIH Grant GM60259-01. MAC would like to acknowledge support from Undergraduate Summer Scholars program. AP acknowledges support from Howard Hughes Grant no. 71199-520403.

References

[1] B. Bechinger, M. Zasloff, S.J. Opella, Biophys. J. 74 (1998) 981–987.
[2] K.P. Howard, S.J. Opella, J. Magn. Reson., Ser. B 112 (1996) 91–94.
[3] R.R. Ketchem, W. Hu, T.A. Cross, Science 261 (1993) 1457–1460 (Washington, D.C., 1883).
[4] Y. Kim, K. Valentine, S.J. Opella, S.L. Schendel, W.A. Cramer, Protein Sci. 7 (1998) 342–348.
[5] S. Lambotte, P. Jasperse, B. Bechinger, Biochemistry 37 (1998) 16–22.
[6] J.A. Losonczi, J.H. Prestegard, Biochemistry 37 (1998) 706–716.
[7] S.J. Opella, Nat. Struct. Biol. 4 (1997) 845–848.
[8] J.H. Prestegard, Nat. Struct. Biol. 5 (1998) 517–522.
[9] F.M. Marassi, A. Ramamoorthy, S.J. Opella, Proc. Natl. Acad. Sci. U. S. A. 94 (1997) 8551–8556.
[10] C.R. Sanders, R.S. Prosser, Structure 6 (1998) 1227–1234.
[11] K.J. Glover, J.A. Whiles, M.J. Wood, G. Melacini, E.A. Komives, R.R. Vold, Biochemistry 40 (2001) 13137–13142.
[12] J.P. Barnes, J.H. Freed, Biophys. J. 75 (1998) 2532–2546.

[13] M. Ge, D.E. Budil, J.H. Freed, Biophys. J. 66 (1994) 1515–1521.
[14] S. Schreier-Muccillo, D. Marsh, H. Duas, H. Schneider, I.C.P. Smith, Chem. Phys. Lipids 10 (1973) 11–27.
[15] P. Jost, L.J. Libertini, V.C. Hebert, O.H. Griffith, J. Mol. Biol. 59 (1971) 77–98.
[16] A. Lange, D. Marsh, K.H. Wassmer, P. Meier, G. Kothe, Biochemistry 24 (1985) 4383–4392.
[17] R.D. Lapper, S.J. Paterson, I.C.P. Smith, Can. J. Biochem. 50 (1972) 969–981.
[18] C. Mailer, C.P.S. Taylor, S. Schreier-Muccillo, I.C.P. Smith, Arch. Biochem. Biophys. 163 (1974) 671–678.
[19] J. Seelig, in: L.J. Berliner (Ed.), Spin Labeling Theory and Applications, Academic Press, New York, 1976, pp. 373–410.
[20] I.C.P. Smith, K.W. Butler, in: L.J. Berliner (Ed.), Spin Labeling Theory and Applications, Academic Press, New York, 1976, pp. 411–453.
[21] H. Tanaka, J.H. Freed, J. Phys. Chem. 88 (1985) 350–360.
[22] C.R. Sanders, B.J. Hare, K.P. Howard, J.H. Prestegard, Prog. NMR Spectrosc. 26 (1994) 421–444.
[23] R.S. Prosser, S.A. Hunt, J.A. DiNatale, R.R. Vold, J. Am. Chem. Soc. 118 (1996) 269–270.
[24] R.S. Prosser, J.S. Hwang, R.R. Vold, Biophys. J. 74 (1998) 2405–2418.
[25] R.S. Prosser, V.B. Volkov, I.V. Shiyanovskaya, Biophys. J. 75 (1998) 2163–2169.
[26] R.S. Prosser, V.B. Volkov, I.V. Shiyanovskaya, Biochem. Cell. Biol. 76 (1998) 443–451.
[27] R.S. Prosser, I.V. Shiyanovskaya, Concepts Magn. Reson. 13 (2001) 19–31.
[28] J.A. Whiles, R. Brasseur, K.J. Glover, G. Melacini, E.A. Komives, R.R. Vold, Biophys. J. 80 (2001) 280–293.
[29] R.R. Vold, R.S. Prosser, J. Magn. Reson., Ser. B 113 (1996) 267–271.
[30] J. Katsaras, R.L. Donaberger, I.P. Swainson, D.C. Tennant, Z. Tun, R.R. Vold, R.S. Prosser, Phys. Rev. Lett. 78 (1997) 899–902.
[31] S.M. Garber, G.A. Lorigan, K.P. Howard, J. Am. Chem. Soc. 121 (1999) 3240–3241.
[32] M.L. Mangels, T.B. Cardon, A.C. Harper, K.P. Howard, G.A. Lorigan, J. Am. Chem. Soc. 122 (2000) 7052–7058.
[33] M. Barranger-Mathys, D.S. Cafiso, Biochemistry 35 (1996) 498–505.
[34] H. Hauser, C.C. Hinckley, J. Krebs, B.A. Levine, M.C. Phillips, R.J.P. Williams, Biochim. Biophys. Acta 468 (1977) 364–377.
[35] J. Conti, H.N. Halladay, M. Petersheim, Biochim. Biophys. Acta 902 (1987) 53–64.
[36] V.S. Mironov, Y.G. Galyametdinov, A. Ceulemans, K. Binnemans, J. Chem. Phys. 113 (2000) 10293–10303.
[37] M.L. Mangels, A.C. Harper, A.I. Smirnov, K.P. Howard, G.A. Lorigan, J. Magn. Reson. 151 (2001) 253–259.
[38] T.B. Cardon, E.K. Tiburu, A. Padmanabhan, K.P. Howard, G.A. Lorigan, J. Am. Chem. Soc. 123 (2001) 2913–2914.
[39] Y. Cheng, B.W. Chen, J.F. Lu, K. Wang, J. Inorg. Biochem. 69 (1998) 1–7.
[40] D. Marsh, V.A. Livshits, Phys. Med. Biol. 43 (1998) 1977–1986.
[41] D. Marsh, Chem. Soc. Rev. 22 (1993) 329–335.
[42] V.A. Livshits, B.G. Dzikovski, D. Marsh, J. Magn. Reson. 148 (2001) 221–237.
[43] C. Altenbach, D.A. Greenhalgh, H.G. Khorana, W.L. Hubbell, Proc. Natl. Acad. Sci. U. S. A. 91 (1994) 1667–1671.
[44] L.A. Dalton, J.O. McIntyre, S. Fleischer, Biochemistry 26 (1987) 2117–2130.
[45] J.S. Leigh, J. Chem. Phys. 52 (1970) 2608–2612.
[46] T. Pali, R. Bartucci, L.I. Horvath, D. Marsh, Biophys. J. 61 (1992) 1595–1602.
[47] J. Reuben, D. Fiat, J. Chem. Phys. 51 (1969) 4918–4927.
[48] R.A. Dwek, H.R. Levy, G.K. Radda, P.J. Seeley, Biochim. Biophys. Acta 377 (1975) 26–33.